East European Journal of Physics. 2. 212-218 (2026)
DOI:10.26565/2312-4334-2026-2-22 ISSN 2312-4334

A SYSTEMATIC ANALYTICAL AND NUMERICAL STUDY OF INCOMPLETE DOPANT IONIZATION IN GERMANIUM OVER 4–400 K

M.Sh. Ibragimova[1]*, D.A. Qalandarova[1], N.P. Babayazova[1], U.G. Salayev[1], D.G. Yulchiev[2], A.B. Tilyakov[3], A.V. Alimov[3], Sh.M. Kuliyev[4], U.S. Rakhmonov[5]
[1]*Urgench State University, Hamid Olimjon Street, 14, Urgench, 220100 Uzbekistan*
[2]*Tashkent Institute of Irrigation and Agricultural Mechanization Engineers, National Research University, Department of Irrigation and Melioration, Tashkent, Uzbekistan*
[3]*Department of Emergency Medicine and Disaster Medicine. Tashkent State Medical University, Uzbekistan*
[4]*S.A. Azimov Physical-Technical Institute of Uzbekistan Academy of Sciences*
[5]*Tashkent State Technical University, Tashkent, Uzbekistan*
**Corresponding Author e-mail: madinabonubahodir2024@gmail.com*
Received January 25, 2026; revised April 3, 2026; accepted April 5, 2026

Incomplete dopant ionization critically influences the electrical properties of germanium (Ge), particularly under low-temperature and low-doping conditions relevant to advanced electronic and optoelectronic devices. In this work, we present a systematic numerical investigation of temperature- and concentration-dependent dopant ionization in Ge over temperature range of 4–400 K and dopant concentrations from 1×10^{14} to 1×10^{18} cm^{-3}. Ionization probabilities are evaluated for common acceptor dopants (Boron, Gallium, and Indium) and donor dopants (Phosphorus, Arsenic, and Antimony), with activation energies spanning 10–16 meV. The results reveal severe dopant freeze-out at cryogenic temperatures, where ionization probabilities drop below 0.1–0.2 for lightly doped Ge ($N \leq 10^{15}$ cm^{-3}), leading to carrier density reductions exceeding 80–90% compared to full-ionization assumptions. Donor dopants with lower activation energies achieve near-complete ionization ($P(T) > 0.9$) at 100–150 K, while higher-energy acceptors require temperatures above 200–250 K. Increasing dopant concentration to 10^{17}–10^{18} cm^{-3} significantly suppresses freeze-out, enabling ionization probabilities above 0.8 at temperatures as low as 50–70 K. At and above room temperature, all dopants exhibit near-unity ionization across the investigated concentration range. These findings provide quantitative guidelines for dopant selection and concentration optimization in Ge-based electronic, optoelectronic, and cryogenic devices, emphasizing the necessity of explicitly accounting for incomplete ionization in low-temperature device modeling and design.
Keywords: *Semiconductor band gap; Germanium (Ge); Doping threshold; Temperature effects; Carrier concentration; Incomplete ionization;*
PACS: 73.40. Lq, 73.61.Cw, 73.61.Ey, 72.20.Jv

INTRODUCTION

Germanium (Ge) has re-emerged as a strategically important semiconductor owing to its superior electronic, optical, and thermal properties, which make it highly attractive for next-generation electronic, photonic, and sensing technologies. Its narrow indirect bandgap (~0.66 eV at 300 K), intrinsically high electron and hole mobilities, and strong infrared absorption enable efficient charge transport and enhanced sensitivity compared to conventional silicon-based devices [1-5]. These properties position Ge at a unique intersection between silicon and III–V semiconductors, supporting high-performance operation over wide temperature ranges.

Recent advances in Si-compatible integration, including SiGe heterostructures and Ge-on-Si platforms, have further accelerated the adoption of Ge in modern microelectronics. The high carrier mobility of Ge significantly improves device performance in high-speed logic and radio-frequency (RF) applications, enabling operation in the GHz–THz regime while maintaining full compatibility with CMOS fabrication processes [2,3]. In optoelectronics, Ge exhibits strong absorption in the near-infrared region (0.8–1.6 μm), coinciding with key telecommunication wavelengths. Consequently, Ge-based p–n, p–i–n, and avalanche photodiodes are widely implemented in silicon photonics, optical interconnects, LiDAR, and fiber-optic communication systems [3–6]. Germanium also plays a critical role in high-efficiency photovoltaic technologies, particularly as a substrate and bottom cell in multi-junction solar cells such as InGaP/GaAs/Ge, enabling superior spectral utilization and power conversion efficiencies beyond the single-junction Shockley–Queisser limit [6]. In addition, Ge exhibits exceptional temperature sensitivity, making it well-suited for precision thermistors, cryogenic sensors, and thermo-optic photonic devices. High-purity germanium (HPGe) detectors further remain the benchmark for gamma-ray and X-ray spectroscopy due to their outstanding energy resolution [1,7].

Despite these advantages, the performance of Ge-based devices is strongly governed by temperature-dependent dopant activation and carrier statistics. In particular, incomplete dopant ionization becomes significant at low and intermediate temperatures, leading to pronounced deviations between the nominal doping concentration and the effective free carrier density [10]. This effect directly impacts conductivity, capacitance–voltage characteristics, and junction electrostatics. While incomplete ionization has been extensively studied in silicon [11-12], GaAs [13-18], and Si/GaAs

Cite as: M.Sh. Ibragimova, D.A. Qalandarova, N.P. Babayazova, U.G. Salayev, D.G. Yulchiev, A.B. Tilyakov, A.V. Alimov, Sh.M. Kuliyev, U.S. Rakhmonov, East Eur. J. Phys. 2, 212 (2026), https://doi.org/10.26565/2312-4334-2026-2-22
© M.Sh. Ibragimova, D.A. Qalandarova, N.P. Babayazova, U.G. Salayev, D.G. Yulchiev, A.B. Tilyakov, A.V. Alimov, Sh.M. Kuliyev, U.S. Rakhmonov, 2026; CC BY 4.0 license

heterostructures [19-25], a systematic and comparative investigation for germanium over wide temperature [26,27] and doping ranges remains notably lacking [28-30], despite its growing importance in cryogenic electronics and thermal sensing [31,32].

In this work, we present a comprehensive analysis of incomplete ionization effects in germanium across a temperature range of 4–400 K and doping concentrations from 10^{15} to 10^{18} cm^{-3}. A comparative study is conducted for common donor (P, As, Sb) and acceptor (B, Ga, In) impurities. By combining analytical modeling based on Fermi–Dirac statistics and charge neutrality with numerical simulations, we elucidate dopant activation mechanisms and their impact on carrier concentration and electro-physical properties. The results provide essential insight and practical guidelines for the accurate modeling and optimization of Ge-based electronic, optoelectronic, and sensing devices operating over broad temperature regimes.

METHODS AND MATERIAL

2.1. Material Parameters and Doping Conditions

Germanium (Ge) is a group IV semiconductor with a diamond cubic (face-centered cubic, FCC) crystal structure and a lattice constant of 5.658 Å. It exhibits an indirect bandgap of 0.66 eV at 300 K, which enables efficient infrared absorption and makes it suitable for photodetector and optoelectronic applications. The effective mass of electrons in Ge is 0.12 m_0, while holes have a heavier mass of 0.29 m_0 for heavy holes and 0.043 m_0 for light holes. These low effective masses contribute to the material's high carrier mobility, approximately 3900 cm²/V·s for electrons and 1900 cm²/V·s for holes at room temperature, allowing fast charge transport in electronic and photonic devices. The intrinsic carrier concentration of Ge is relatively low, around 2.4×10^{13} cm^{-3} at 300 K, which ensures low leakage currents in p-n junction devices. Germanium also has a high relative permittivity of 16.2, which reduces the depletion width for a given doping level, enabling compact device geometries. Its thermal conductivity is 60 W/m·K, supporting efficient heat dissipation, and the material has a density of 5.323 g/cm³ with a melting point of 938 °C, setting processing limits for high-temperature fabrication. Germanium's narrow bandgap, high carrier mobility, and favorable permittivity make it an excellent choice for high-speed electronics, infrared photodetectors, and advanced optoelectronic devices. Moreover, the material allows the formation of ohmic contacts with low-resistance metal interfaces, which is essential for efficient current injection and extraction in diodes, LEDs, and photodetectors. Collectively, these properties underpin the superior performance of Ge-based semiconductor devices in both electronic and optoelectronic applications.

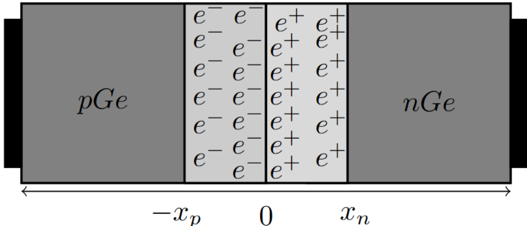

Figure 1. Schematic p-n junction in Germanium (Ge)

Figure 1 illustrates a p-n junction in germanium (Ge) with clearly marked ohmic contacts at the edges and the depletion region at the junction interface. The left region (pGe) is p-type, rich in holes (e^-), while the right region (nGe) is n-type, rich in electrons (e^+). The central depletion region extends from $-x_p$to x_n, where mobile carriers are swept away, leaving fixed ionized donors and acceptors, creating a built-in electric field.

Table 1. Donor and acceptor dopants in germanium and their key parameters

Acceptor (meV)	Boron (B) E_A=10	Gallium (Ga) E_A=12	Indium (In) E_A=16
Donor (meV)	Phosphorus (P) E_D=12	Arsenic (As) E_D=14	Antimony (Sb) E_D=10

The black rectangles at both ends represent ohmic contacts, ensuring low-resistance electrical connection to the external circuit. These contacts allow current injection and extraction without introducing additional potential barriers, which is crucial for device performance. Within the depletion region, the alternating $e^-$and e^+symbols depict electron-hole separation. This separation underpins the rectifying behavior of the junction, as the internal field opposes further carrier diffusion. The gray shading distinguishes the neutral regions, where majority carriers dominate, from the partially depleted regions near the junction. Figure 1 effectively shows a Ge p-n junction with ohmic contacts, illustrating carrier distribution, depletion width, and the electric field, providing a fundamental understanding of semiconductor device operation.

2.2 Analytical Modeling of Temperature-Dependent Ionization

The behavior of p–n junctions in germanium (Ge) was analytically modeled by solving Poisson's equation under the depletion approximation, explicitly including temperature-dependent incomplete dopant ionization. For a three-dimensional structure, the electric field $\mathrm{E}(r)$is assumed uniform along the lateral directions, and varies only along the junction axis, yielding (1):

$$\frac{dE(r)}{dr}=\frac{\partial E(x,y,z)}{\partial x}+\frac{\partial E(x,y,z)}{\partial y}+\frac{\partial E(x,y,z)}{\partial z}=\frac{\rho(x,y,z)}{\varepsilon\cdot\varepsilon_0} \tag{1}$$

Where $\varepsilon=16.2$ is the relative permittivity of Ge, $\varepsilon_0\approx$ $8.854\cdot10^{12}$ F/m is the vacuum permittivity, and $\rho(r,T)$is the space charge density, defined as (2):

$$\rho(r,T)=q\cdot(p(r)-n(r)+N_D^+(T)-N_A^-(T)) \tag{2}$$

with $q=1.602\cdot10^{-19}\ C$, $p(r)$and $n(r)$the hole and electron concentrations, and $N_D^+(T)$, $N_A^-(T)$the ionized donor and acceptor densities. The ionized dopant concentrations are described using Fermi–Dirac statistics corrected for the temperature-dependent density of states. The probabilities of ionization for acceptor $P_A(T)$ and donor $P_D(T)$ dopants are directly related to the fraction of ionized dopants in the material. They are defined using equations (3a) and (3b) as:

$$\begin{cases} P_A(T)=\dfrac{1}{1+\dfrac{g_A\cdot p_p(r)}{\gamma_p(T)\cdot N_V(T)}\cdot\exp\left(\dfrac{\Delta E_A}{kT}\right)} & (3a) \\ P_D(T)=\dfrac{1}{1+\dfrac{g_D\cdot n_n(r)}{\gamma_n(T)\cdot N_C(T)}\cdot\exp\left(\dfrac{\Delta E_D}{kT}\right)} & (3b) \end{cases}$$

where $g_D=4, g_A=2$ are the dopant degeneracy factors, $N_C(T)$and $N_V(T)$are the effective density of states in the conduction and valence bands, and $\Delta E_D$and $\Delta E_A$are the dopant activation energies. For example, common dopants in Ge have the following activation energies: To bridge the quantum Fermi–Dirac statistics with classical Maxwell–Boltzmann approximations, temperature-dependent correction factors $\gamma_n(T)$and $\gamma_p(T)$were introduced, ensuring a physically consistent description of both majority carrier concentrations and dopant ionization over the entire 4–400 K range. This analytical framework allows precise calculation of temperature-dependent carrier densities, $n(T)$and $p(T)$, capturing freeze-out, partial ionization, and full ionization regimes. It provides a quantitative foundation for designing Ge-based electronic and optoelectronic devices, including photodetectors and low-temperature sensors, by predicting the effective free carrier density as a function of both temperature and dopant concentration. $\Delta E_D=E_C-E_D$, $\Delta E_A=E_A-E_V$ activation energy donor and acceptor, with donor and acceptor energy levels E_D and E_A facilitating n-type and p-type conductivity respectively, as shown in Figure 2.

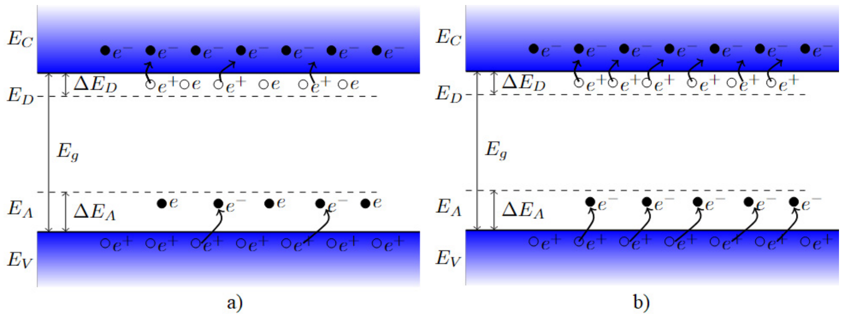

Figure. 2. Schematic illustration of the band diagrams for acceptors and donors:
(a) partially ionized state at low temperatures and (b) fully ionized state at high temperatures

In Figure 2 b) at high temperatures, donor atoms (such as phosphorus in Si) are fully ionized, donating electrons to the conduction band and thereby enhancing the material's electrical conductivity. Similarly, acceptor atoms (like boron in Si) ionize by accepting electrons from the valence band, creating holes that also contribute to conductivity. In contrast, Figure 2 a) shows that at low temperatures below 20 K, incomplete ionization occurs, where not all donor and acceptor atoms ionize.

RESULTS AND DISCUSSION

The temperature-dependent ionization of acceptor (B, Ga, In) and donor (P, As, Sb) dopants in lightly doped germanium ($N_A=N_D=1\times10^{15}\ \text{cm}^{-3}$) exhibits pronounced freeze-out at cryogenic temperatures and near-complete ionization above room temperature. At $T<50$ K, high-energy dopants such as Indium and Arsenic remain largely inactive ($P<0.1$), while low-energy dopants like Boron and Antimony begin ionizing earlier, highlighting the strong sensitivity of ionization to activation energy. In the intermediate range (50–150 K), ionization rapidly increases, with donors generally ionizing at lower temperatures than acceptors due to higher degeneracy and conduction-band density of states. Temperature–concentration maps reveal that low dopant densities exacerbate freeze-out, whereas increasing dopant

concentration partially mitigates incomplete ionization, though cryogenic suppression persists even at $N \sim 10^{18}$ cm^{-3}. These results underscore that dopant selection critically impacts low-temperature device performance, with low-activation-energy species preferred for cryogenic sensors, detectors, and quantum devices. Incorporating temperature-dependent effective densities of states and incomplete ionization in models is essential for accurate prediction of carrier density, depletion width, and current transport, enabling optimized design of Ge-based electronic and optoelectronic systems across 4–400 K.

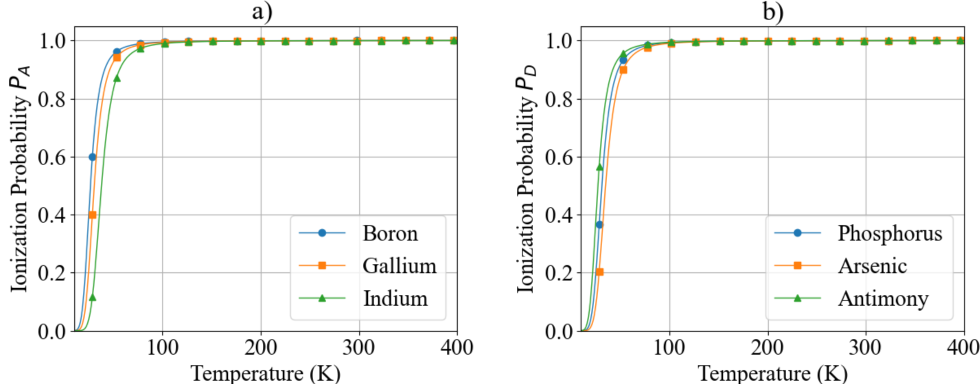

Figure 3. Ionization Probabilities of Dopants in Germanium (Ge) (a) Acceptor Ionization Probability $P_A(T)$ for Boron, Gallium, and Indium (b) Donor Ionization Probability $P_D(T)$ for Phosphorus, Arsenic, and Antimony

Figure 3 illustrates the temperature dependence of dopant ionization probability in lightly doped germanium, with equal acceptor and donor concentrations of $N_A = N_D = 1 \times 10^{15}$ cm^{-3}. Representative shallow acceptor (B, Ga, In) and donor (P, As, Sb) species are considered. The calculations are based on an analytical Fermi–Dirac ionization model that explicitly incorporates temperature-dependent effective densities of states, $N_V(T)$and $N_C(T)$, as well as dopant-specific activation energies. Figure 3(a): Acceptor Dopants: Figure 3(a) presents the ionization probability $P_A(T)$of Boron (10 MeV), Gallium (12 meV), and Indium (16 meV) over the temperature range 4–400 K. At cryogenic temperatures (T < 40 K), all acceptors are in the freeze-out regime, exhibiting very low ionization probabilities ($P_A < 0.1$). At 10 K, Boron reaches $P_A \approx 0.12$, Gallium $P_A \approx 0.08$, while Indium remains below $P_A \approx 0.04$, highlighting the strong sensitivity of ionization to acceptor activation energy. In the intermediate temperature range (50–150 K), a rapid increase in ionization probability is observed. Boron achieves $P_A > 0.9$ at approximately 120 K, Gallium near 150 K, whereas Indium requires temperatures exceeding 200 K to reach comparable ionization levels. This temperature shift of roughly 80 K between Boron and Indium directly reflects their 6 meV difference in activation energy. At temperatures $T \geq 250$K, all acceptors are essentially fully ionized ($P_A > 0.98$), confirming the validity of the complete ionization assumption for lightly doped Ge at and above room temperature. Figure 3(b): Donor Dopants: Figure 3(b) shows the donor ionization probability $P_D(T)$for Phosphorus (12 meV), Arsenic (14 meV), and Antimony (10 meV). At low temperatures ($T < 40$K), donor ionization is likewise strongly suppressed, with $P_D < 0.15$for all species. Antimony, having the lowest donor activation energy, exhibits the highest ionization probability, reaching $P_D \approx 0.18$at 20 K, compared to $P_D \approx 0.10$for Phosphorus and below 0.07 for Arsenic. Within the intermediate temperature range (80–150 K), donors ionize more rapidly than acceptors. Antimony reaches $P_D \approx 0.9$at approximately 100 K, Phosphorus near 130 K, and Arsenic around 160 K. Above 200 K, all donor species exhibit near-unity ionization ($P_D > 0.99$). Overall, Figure 3 demonstrates that donor dopants in Ge ionize at slightly lower temperatures than acceptors with comparable activation energies. This behavior arises primarily from differences in degeneracy factors ($g_D = 4$ for donors versus $g_A = 2$for acceptors) and the larger effective density of states in the conduction band. At low temperatures, incomplete dopant ionization dominates the electrical behavior of germanium, particularly in lightly doped material (1×10^{15} cm^{-3}), where the free carrier density may be reduced by up to 90% below 50 K. As temperature increases, the system transitions from the freeze-out regime (strongly suppressed ionization) to a partial ionization regime, and ultimately to full ionization at higher temperatures ($T > 300$ K). The dopant activation energy determines the temperature range over which these regimes occur. High-energy dopants such as Indium and Arsenic exhibit delayed ionization and more pronounced freeze-out, while low-energy dopants such as Boron and Antimony ionize at lower temperatures and provide higher carrier concentrations under cryogenic conditions. This behavior is especially critical for germanium-based low-temperature sensors, radiation detectors, and quantum electronic devices. The temperature-dependent ionization characteristics shown in Figure 3 have important implications for Ge-based device design: Cryogenic electronics and sensors: Low-activation-energy dopants (e.g., B and Sb) are preferred to minimize carrier freeze-out and maintain adequate conductivity at low temperatures. Optoelectronic and room-temperature devices: At moderate and room temperatures, the choice of dopant becomes less critical, as nearly complete ionization is achieved for all species. Analytical and numerical device modeling: Accurate inclusion of temperature-dependent $N_C(T)$, $N_V(T)$, and incomplete ionization effects is essential for predicting free carrier density, depletion width, capacitance, and current–voltage characteristics in Ge p–n junctions and MOS devices. At 77 K, Boron exhibits an ionization probability of approximately 20%, while Indium remains below 10%. Among donors,

Antimony achieves approximately 25% ionization at 77 K, whereas Arsenic remains below 10%. At 300 K, all dopants are nearly fully ionized (> 90%), validating the commonly used assumption of complete ionization for lightly doped germanium at room temperature. These results highlight the critical role of incomplete dopant ionization at cryogenic temperatures and provide quantitative guidance for selecting dopant species and concentrations in low-temperature Ge-based electronic and optoelectronic devices.

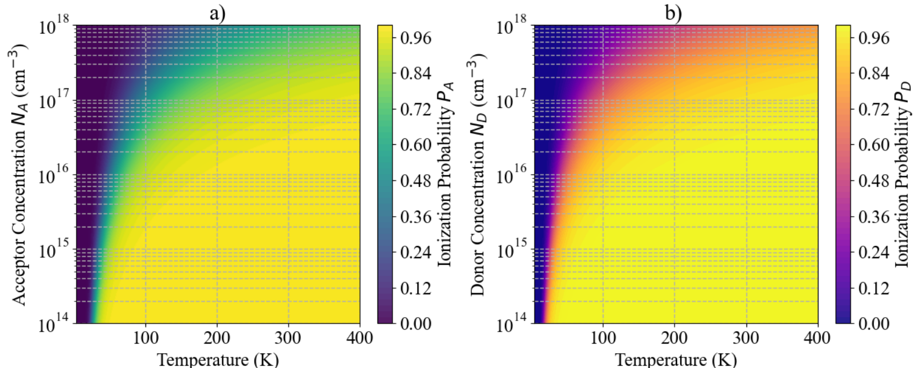

Figure 4. Temperature- and concentration-dependent ionization probabilities of dopants in Germanium
(a) Acceptor ionization probability $P_A(T, N_A)$for Boron, Gallium, and Indium over 4–400 K and 10^{14}–10^{18} cm^{-3}; (b) Donor ionization probability $P_D(T, N_D)$for Phosphorus, Arsenic, and Antimony over the same ranges. Color maps indicate the fraction of ionized dopants, with low temperatures and low concentrations showing pronounced freeze-out.

Figure 4 extends the analysis by mapping ionization probability as a function of both temperature (4–400 K) and dopant concentration (1×10^{14}–1×10^{18} cm^{-3}), providing a comprehensive picture of incomplete ionization effects. Figure 4(a): Acceptor Dopants Figure 4(a) shows contour maps of acceptor ionization probability $P_A(T, N_A)$for Boron, Gallium, and Indium. At low temperatures (<50 K) and low concentrations ($N_A \leq 10^{15}$ cm^{-3}), ionization probabilities remain below 0.2, indicating severe freeze-out. For example, at 20 K and 10^{14} cm^{-3}, Boron exhibits $P_A \approx 0.15$, while Indium remains below $P_A \approx 0.05$. As dopant concentration increases, freeze-out is partially mitigated. At $N_A = 10^{17}$ cm^{-3}, Boron achieves $P_A > 0.7$already at 50 K, whereas Indium still requires temperatures above 120 K to exceed the same ionization level. This illustrates how higher activation energy dopants remain sensitive to freeze-out even at elevated concentrations. At T ≥ 300 K, all acceptors reach $P_A > 0.95$across the entire concentration range, indicating that thermal ionization dominates over concentration-dependent effects. Figure 4(b): Donor Dopants Figure 4(b) presents donor ionization probability $P_D(T, N_D)$for Phosphorus, Arsenic, and Antimony. At 10–30 K and $N_D < 10^{15}$ cm^{-3}, ionization remains below 0.2 for all donors, with Antimony showing the highest ionization fraction. At $N_D = 10^{16}$ cm^{-3}and 50 K, Antimony reaches $P_D \approx 0.8$, while Arsenic remains near $P_D \approx 0.5$. Donor dopants achieve near-complete ionization at lower temperatures than acceptors. For concentrations above 10^{17} cm^{-3}, all donors reach $P_D > 0.95$by 150–180 K, whereas acceptors require temperatures closer to 200–250 K, particularly for Indium. At room temperature (300 K), donors are fully ionized ($P_D > 0.99$) across the entire concentration range, confirming robust carrier activation for n-type Ge devices. Comparative Implications for Device Design Figure 3 isolates the intrinsic temperature dependence and highlights the activation-energy-controlled onset of ionization in lightly doped Ge. Figure 4 demonstrates that dopant concentration can partially compensate for freeze-out, but does not eliminate activation-energy limitations at cryogenic temperatures. Donors consistently ionize at lower temperatures than acceptors, making n-type Ge more suitable for low-temperature electronics. At 50–100 K, carrier densities can be reduced by 70–90% relative to full ionization assumptions for $N < 10^{15}$ cm^{-3}, significantly impacting conductivity and junction behavior. Figures 3 and 4 collectively show that incomplete dopant ionization is a dominant limiting factor in germanium at low temperatures and low doping concentrations. While room-temperature operation (300–500 K) ensures stable and nearly complete ionization, cryogenic operation requires careful dopant selection and concentration optimization. Future work should incorporate heterostructure band alignment, impurity band formation, interface states, and experimental validation, particularly for size-engineered and low-temperature Ge-based optoelectronic and sensing devices.

CONCLUSIONS

In this work, we presented a comprehensive numerical analysis of temperature- and concentration-dependent dopant ionization in germanium, covering temperatures from 4 to 400 K and dopant concentrations spanning $1 \times 10^{14}$to 1×10^{18} cm^{-3}. The results clearly demonstrate that incomplete dopant ionization is a dominant factor governing free-carrier availability in Ge, particularly under low-temperature and low-doping conditions. For lightly doped material ($N = 1 \times 10^{15}$ cm^{-3}), both acceptor and donor species exhibit pronounced freeze-out below 40–50 K, where ionization probabilities fall below 0.1–0.2, corresponding to a reduction of electrically active carriers by more than 80–90% compared to full-ionization assumptions. Donor dopants with low activation energies, such as antimony ($E_D = 10$ meV), reach an ionization probability of $P_D > 0.9$at temperatures of approximately 100–120 K, whereas higher-energy donors such as arsenic ($E_D = 14$ meV) require temperatures exceeding 150–170 K to achieve similar activation. In contrast,

acceptor dopants exhibit slower ionization, with boron ($E_A = 10$ meV) reaching $P_A \approx 0.9$near 120–140 K, while indium ($E_A = 16$ meV) requires temperatures above 220–250 K. The combined temperature–concentration analysis reveals that increasing dopant concentration to 10^{17}–10^{18} cm^{-3}significantly mitigates freeze-out effects. At these concentrations, low-activation-energy dopants exhibit ionization probabilities exceeding 0.8 at temperatures as low as 50–70 K. Nevertheless, even at the highest investigated concentrations, incomplete ionization persists below 30 K, indicating that impurity activation remains thermally limited in cryogenic regimes. At elevated temperatures (300–400 K), all dopant species achieve near-complete ionization ($P > 0.95$–0.99) across the full concentration range, confirming the validity of full-ionization approximations for conventional room-temperature and high-temperature Ge-based devices. However, the results emphasize that such assumptions are no longer valid for low-temperature electronics, infrared detectors, and cryogenic sensing applications, where carrier densities, resistivity, and junction characteristics can deviate by more than an order of magnitude if incomplete ionization is neglected. Overall, this study provides quantitative design guidelines for dopant selection and concentration optimization in germanium, highlighting the necessity of incorporating temperature- and concentration-dependent ionization models for accurate prediction and optimization of electronic and optoelectronic device performance across broad temperature ranges.

ORCID

Madinabonu Sh. Ibragimova, https://orcid.org/0009-0004-7867-7086; **Dildora A. Qalandarova,** https://orcid.org/0009-0005-5130-464X; **Nazokat P. Babayazova,** https://orcid.org/0009-0006-7877-2459; **Ulug'bek G. Salayev,** https://orcid.org/0009-0001-8223-1114; **Davronbek Gulamovich Yulchiev,** https://orcid.org/0000-0002-9251-2710; **Aziz Burievich Tilyakov,** https://orcid.org/0000-0002-9743-0482; **Akhbor Valievich Alimov,** https://orcid.org/0009-0003-0491-650X; **Shukur M. Kuliyev,** https://orcid.org/0009-0006-7692-3954; **Uktam Sodikovich Rakhmonov,** https://orcid.org/0000-0001-8926-9505

REFERENCES

[1] N. Abrosimov, M. Czupalla, N. Dropka, J. Fischer, A. Gybin, K. Irmscher, J. Janicskó-Csáthy, *et al*., "Technology development of high purity germanium crystals for radiation detectors," Journal of Crystal Growth, **532**, 125396 (2020). https://doi.org/10.1016/j.jcrysgro.2019.125396

[2] Sh.B. Utamuradova, Sh.Kh. Daliev, J.J. Khamdamov, Kh.J. Matchonov, M.K. Karimov, and Kh.Y. Utemuratova, East Eur. J. Phys. (1), 276 (2025), https://doi.org/10.26565/2312-4334-2025-1-32

[3] D.A. Kozak, N.F. Tyndall, M.W. Pruessner, W.S. Rabinovich, and T.H. Stievater, "Germanium-on-silicon waveguides for long-wave integrated photonics: Ring resonance and thermo-optics," Optics Express, **29**(10), 15443–15451 (2021). https://doi.org/10.1364/OE.420687

[4] A. Torres, M. Moreno, A. Kosarev, and A. Heredia, "Thermo-sensing silicon–germanium–boron films prepared by plasma for un-cooled micro-bolometers," Journal of Non-Crystalline Solids, **354**(19–25), 2556–2560 (2008). https://doi.org/10.1016/j.jnoncrysol.2007.09.112

[5] Z. Wu, S. Wang, J. Jiang, K. Liu, and T. Liu, "High-sensitivity temperature sensor based on microsphere cavity in super larger thermo-optic coefficient germanium-core fiber," IEEE Access, 7, 182658–182663 (2019). https://doi.org/10.1109/ACCESS.2019.2960178

[6] C.S. Mishra, "Temperature-dependent nonlinear optical behavior of germanium semiconductor structures for infrared sensing applications," IEEE Journal of Selected Topics in Quantum Electronics, **31**(6), 4400108 (2025). https://doi.org/10.1109/JSTQE.2025.3596090

[7] J. Feng, Z. Zhang, J. Liu, M. Shao, and Y. Zhou, "A novel resistive anode using a germanium film for Micromegas detectors," Nuclear Instruments and Methods in Physics Research Section A, **1031**, 166595 (2022). https://doi.org/10.1016/j.nima.2022.166595

[8] M. Patel, and A.K. Karamalidis, "Germanium: A review of its US demand, uses, resources, chemistry, and separation technologies," Separation and Purification Technology, **275**, 118981 (2021). https://doi.org/10.1016/j.seppur.2021.118981

[9] J.Sh. Abdullayev, and I.B. Sapaev, "Optimization of the influence of temperature on the electrical distribution of structures with radial p-n junction structures," East European Journal of Physics, (3), 344–349 (2024). https://doi.org/10.26565/2312-4334-2024-3-39

[10] J.Sh. Abdullayev, and I.B. Sapaev, "Optimizing the Influence of Doping and Temperature on the Electrophysical Features of p-n and p-i-n Junction Structures," Eurasian Physical Technical Journal, **21**(3(49)), 21–28 (2024). https://doi.org/10.31489/2024No3/21-28

[11] J.Sh. Abdullayev, I.B. Sapaev, and Kh.N. Juraev, "Theoretical analysis of incomplete ionization on the electrical behavior of radial p-n junction structures," Low Temperature Physics, **51**, 60–64 (2025). https://doi.org/10.1063/10.0034646

[12] J.Sh. Abdullayev, and I.B. Sapaev, "Factors influencing the ideality factor of semiconductor p-n and p-i-n junction structures at cryogenic temperatures," East European Journal of Physics, (4), 329–333 (2024). https://doi.org/10.26565/2312-4334-2024-4-37

[13] C.D. Thurmond, "The standard thermodynamic functions for the formation of electrons and holes in Ge, Si, GaAs, and GaP," Journal of The Electrochemical Society, **122**(8), 1133 (1975). https://doi.org/10.1149/1.2134410

[14] J.Sh. Abdullayev, and I.B. Sapaev, "Modeling and calibration of electrical features of p-n junctions based on Si and GaAs," Physical Sciences and Technology, **11**(3–4), 39–48 (2024). https://doi.org/10.26577/phst2024v11i2b05

[15] J.Sh. Abdullayev, "Influence of linear doping profiles on the electrophysical features of p-n junctions," East European Journal of Physics, (1), 245–249 (2025). https://doi.org/10.26565/2312-4334-2025-1-26

[16] P.K. Saxena, P. Srivastava, and A. Srivastava, "Defect analysis of MBE reactor-grown HgCdTe on Si, GaAs, GaSb, and CZT substrates through the TNL-Epigrow simulator," Journal of Electronic Materials, **53**, 5803–5812 (2024). https://doi.org/10.1007/s11664-024-11082-0

[17] J.Sh. Abdullayev, and I.B. Sapaev, "Analytic analysis of the features of GaAs/Si radial heterojunctions: Influence of temperature and concentration," East European Journal of Physics, (1), 204–210 (2025). https://doi.org/10.26565/2312-4334-2025-1-21

[18] J.Sh. Abdullayev, I.B. Sapaev, N. Esanmuradova, S. Kadirov, and S. Kuliyev, "Mathematical analysis of the features of radial p-n junction: Influence of temperature and concentration," East European Journal of Physics, (2), 220–225 (2025). https://doi.org/10.26565/2312-4334-2025-2-24
[19] J.Sh. Abdullayev, I.B. Sapaev, and S.R. Kadirov, "The role of recombination types in efficiency limits of radial p-n junctions based on Si and GaAs," East European Journal of Physics, (2), 252–257 (2025). https://doi.org/10.26565/2312-4334-2025-2-30
[20] I. Sapaev, B. Sapaev, D. Abdullaev, J. Abdullayev, A. Umarov, R. Siddikov, A. Mamasoliev, and K. Daliev, "Influence of the parameters to transition capacitance at NCDS-PSI heterostructure," E3S Web of Conferences, 383(04022), 1–7 (2023). https://doi.org/10.1051/e3sconf/202338304022
[21] J.Sh. Abdullayev, I.B. Sapaev, J.S. Abdullayev, D.A. Juraev, M.J. Jalalov, and E.E. Elsayed, "Mathematical Modeling of Incomplete Ionization in Radial p-Si/n-GaAs Heterojunctions: Temperature and Doping Effects," J. Electron. Mater. **54**, 10484–10492 (2025). https://doi.org/10.1007/s11664-025-12391-8
[22] I.B. Sapaev, J.I. Razzokov, J.S. Abdullayev, D.A. Qalandarova, and M.S. Ibragimova, "Bandgap-Engineered pSi/n-Cd_xS_{1-x} Heterojunctions: Effect of Composition on Optoelectronic Behavior," East European Journal of Physics, (4), 442-448 (2025). https://doi.org/10.26565/2312-4334-2025-4-44
[23] J.Sh. Abdullayev, D.A. Qalandarova, M.Sh. Ibragimova, I.B. Sapaev, and J.I. Razzokov, "Experimental and Simulation-Based Investigation of p-Si/n-CdS Heterojunctions: From Cryogenic Freeze-Out to Room Temperature Operation," J. Electron. Mater. **55**, 2229–2239 (2026). https://doi.org/10.1007/s11664-025-12642-8
[24] A. Kumar, G. Kumar, and C. Kumar, "Design and Performance Evaluation of a $Ge_{1-x}Sn_x$/Ge Multiple Quantum Well Heterojunction Phototransistor for Long-Haul DWDM Optical Communication Systems," J. Electron. Mater. **55**, 3185–3202 (2026). https://doi.org/10.1007/s11664-025-12653-5
[25] Sh.B. Utamuradova, Sh.Kh. Daliev, J.J. Khamdamov, Kh.J. Matchonov, A.Kh. Khaitbaev, East Eur. J. Phys. (4), 484 (2025). https://doi.org/10.26565/2312-4334-2025-4-49
[26] J.Sh. Abdullayev, L. Abdullayeva, L. Agamalieva, and R. Ismailova, "Correlating Ni microstructure with Schottky barrier homogeneity in monolayer MoS_2 field-effect transistors," Advanced Physical Research, **7**(3), 350–357 (2025). https://doi.org/10.62476/apr.73350
[27] J. Sadullayev, M. Akhmedov, M. Vapayev, I. Davletov, and G. Boltaev, "Modeling of Thermal Effects in a Polyimide Target Under Pulsed Laser Irradiation," East European Journal of Physics, (1), 274-280 (2026). https://doi.org/10.26565/2312-4334-2026-1-31
[28] O. Toktarbaiuly, M. Baisariyev, A. Kaisha, T. Duisebayev, N.K. Ibrayev, T. Serikov, M. Ibraimov, *et al*., Eurasian Physical Technical Journal, **21**(4), 131–139 (2024). https://doi.org/10.31489/2024No4/131-139
[29] J.Sh. Abdullayev, D.A. Qalandarova, and M.Sh. Ibragimova, "Impact of incomplete ionization on the critical electric field of p–n junction structures based on Si and GaAs," Low Temperature Physics, **52**(2), 164–169 (2026). https://doi.org/10.1063/10.0042291
[30] O. Toktarbaiuly, A. Syrlybekov, N. Nuraje, G. Sugurbekova, and I.V. Shvets, "Surface faceting of vicinal $SrTiO_3$(100)," Materials Today: Proceedings, **71**(Part 1), 69–77 (2022). https://doi.org/10.1016/j.matpr.2022.08.283
[31] J.S. Abdullayev, M.S. Ibragimova, J.S. Abdullayev, and I.B. Sapaev, "Cryogenic material and electrophysical changes in Si and GaAs," East European Journal of Physics, (1), 343–350 (2026). https://doi.org/10.26565/2312-4334-2026-1-40
[32] J.S. Abdullayev, M.S. Ibragimova, J.S. Abdullayev, and I.B. Sapaev, "Thermal expansion characteristics of planar and radial Si/GaAs p–n heterojunctions," East European Journal of Physics, (1), 388–395 (2026). https://doi.org/10.26565/2312-4334-2026-1-46

СИСТЕМАТИЧНЕ АНАЛІТИЧНЕ ТА ЧИСЕЛЬНЕ ДОСЛІДЖЕННЯ НЕПОВНОЇ ІОНІЗАЦІЇ ДОМІШОК У ГЕРМАНІЇ В ДІАПАЗОНІ ТЕМПЕРАТУР 4–400 К

М.Ш. Ібрагімова[1], Д.А. Каландарова[1], Н.П. Бабаязова[1], У.Г. Салаєв[1], Д.Г. Юльчієв[2], А.Б. Тіляков[3], А.В. Алімов[3], Ш.М. Кулієв[4], У.С. Рахмонов[5]

[1]*Ургенчський державний університет, вулиця Хаміда Олімджона, 14, Ургенч, 220100 Узбекистан*
[2]*Ташкентський інститут інженерів іригації та механізації сільського господарства, Національний дослідницький університет, кафедра іригації та меліорації, Ташкент, Узбекистан*
[3]*Кафедра невідкладної медицини та медицини катастроф. Ташкентський державний медичний університет, Узбекистан*
[4]*Фізико-технічний інститут імені С.А. Азімова Академії наук Узбекистану*
[5]*Ташкентський державний технічний університет, Ташкент, Узбекистан*

Неповна іонізація домішок суттєво впливає на електричні властивості германію (Ge), особливо за умов низьких температур і низького рівня легування, що є критичним для сучасних електронних та оптоелектронних пристроїв. У цій роботі наведено систематичне чисельне дослідження температурної та концентраційної залежності іонізації домішок у Ge в діапазоні температур 4–400 К та за концентрацій домішок від 1×10^{14}до 1×10^{18} см$^{-3}$. Імовірності іонізації оцінено для типових акцепторних домішок (бор, галій, індій) і донорних домішок (фосфор, миш'як, сурма) з енергіями активації в межах 10–16 меВ. Результати демонструють виражений ефект «заморожування» домішок за кріогенних температур, коли імовірність іонізації зменшується до 0,1–0,2 для слаболегованого Ge ($N \leq 10^{15}$ см$^{-3}$), що призводить до зниження концентрації носіїв заряду більш ніж на 80–90% порівняно з припущенням повної іонізації. Донорні домішки з меншою енергією активації досягають майже повної іонізації ($P(T) > 0.9$) при температурах 100–150 К, тоді як акцепторні домішки з вищою енергією активації потребують температур вище 200–250 К. Збільшення концентрації домішок до 10^{17}–10^{18} см$^{-3}$істотно послаблює ефект заморожування, забезпечуючи імовірність іонізації понад 0.8 вже при температурах 50–70 К. За кімнатної температури та вище всі досліджені домішки демонструють майже повну іонізацію в усьому діапазоні досліджених концентрацій. Отримані результати надають кількісні рекомендації щодо вибору типу та концентрації домішок для Ge-базованих електронних, оптоелектронних і кріогенних пристроїв та підкреслюють необхідність явного врахування неповної іонізації домішок під час моделювання та оптимізації пристроїв, що працюють за низьких температур.

Ключові слова: *ширина забороненої зони напівпровідника; германій (Ge); поріг легування; температурні ефекти; концентрація носіїв заряду; неповна іонізація; оптимізація пристроїв*